An iterative Re-uniform method for the numerical solution of the Prandtl boundary-layer problem.*

P. A. Farrell† Alan F. Hegarty‡ John J. H. Miller§

Eugene O'Riordan¶ G. I. Shishkin ||

Abstract. *Prandtl's boundary value problem on a flat plate for a system of boundary layer equations is quasilinear. The solution of such a problem has complicated behaviour. Experience in constructing satisfactory numerical methods for problems with a parabolic boundary layer allows us to develop a "natural" special finite difference scheme for the Prandtl problem; if it is assumed that the coefficients multiplying the derivatives in the transport equation for Prandtl's problem are known, then we have a linear transport equation, and under appropriate conditions on these coefficients, the scheme for Prandtl's problem converges ε-uniformly, where $\varepsilon = Re^{-1}$, and Re is the Reynolds number. It should be noted that at present ε-uniformly convergent difference schemes for Prandtl's problem are unknown. Nevertheless, it is of great interest to study numerically the above-mentioned special scheme. Numerical experiments indicate ε-uniform convergence, with respect to both the number of grid nodes and the number of iterations required for convergence of the iterative process, of both the numerical solution and its discrete derivatives, outside a neighbourhood of the leading edge of the plate.*

*This research was supported in part by the National Science Foundation grant DMS-9627244, by the Enterprise Ireland grant SC-98-612 and by the Russian Foundation for Basic Research under grant No. 98-01-00362.

†Department of Mathematics and Computer Science, Kent State University, Kent, Ohio 44242, U.S.A.

‡Department of Mathematics and Statistics, University of Limerick, Limerick, Ireland

§Department of Mathematics, Trinity College, Dublin 2, Ireland

¶Department of Mathematics, Dublin City University, Dublin 9, Ireland

||Institute of Mathematics and Mechanics, Russian Academy of Sciences, Ural Branch, Ekaterinburg 620219, Russia.

1 Introduction

In this paper we discuss the steady laminar flow of an incompressible fluid on both sides of a thin flat semi–infinite plate $P = \{(x,0) \in \mathbb{R}^2 : x \geq 0\}$. Our goal is to model the flow for all Reynolds numbers for which the flow remains laminar and no separation occurs on the plate. In what follows we determine numerical values of the flow variables and their scaled derivatives. We show, by means of extensive numerical experiments, that our numerical approximations are pointwise accurate and that they satisfy pointwise error estimates that are uniform with respect to the Reynolds number.

Incompressible flow past the plate P in the domain $D = \mathbb{R}^2 \setminus P$ is governed by the Navier–Stokes equations. In this case they can be written in the form

$$(P_{\rm NS}) \begin{cases} \text{Find } \mathbf{u}_{\rm NS} = (u_{\rm NS}, v_{\rm NS}),\ p_{\rm NS} \text{ such that for all } (x,y) \in D, \\ -\frac{1}{Re}\Delta \mathbf{u}_{\rm NS} + \mathbf{u}_{\rm NS} \cdot \nabla \mathbf{u}_{\rm NS} = -\frac{1}{\rho}\nabla p_{\rm NS} \\ \nabla \cdot \mathbf{u}_{\rm NS} = 0 \\ \mathbf{u}_{\rm NS}(x,0) = \mathbf{0} \quad \text{for all } x \geq 0 \\ \lim_{|y|\to\infty} \mathbf{u}_{\rm NS}(x,y) = \lim_{x\to-\infty} \mathbf{u}_{\rm NS}(x,y) = (u_\infty, 0), \quad \text{for all } x \in \mathbb{R} \end{cases}$$

where u_∞ is a constant. This is a nonlinear system of three equations for the three unknowns $\mathbf{u}_{\rm NS}, p_{\rm NS}$. The approach of Prandtl [5], which is described in [1], simplifies $(P_{\rm NS})$ to the following Prandtl problem in the domain D.

$$(P_{\rm P}) \begin{cases} \text{Find } \mathbf{u}_{\rm P} = (u_{\rm P}, v_{\rm P}) \text{ such that for all } (x,y) \in D \\ -\dfrac{1}{Re}\dfrac{\partial^2 u_{\rm P}(x,y)}{\partial y^2} + \mathbf{u}_{\rm P} \cdot \nabla u_{\rm P}(x,y) = 0 \\ \nabla \cdot \mathbf{u}_{\rm P}(x,y) = 0 \\ \mathbf{u}_{\rm P}(x,0) = \mathbf{0} \quad \text{for all } x \geq 0 \\ \lim_{|y|\to\infty} \mathbf{u}_{\rm P}(x,y) = \lim_{x\to-\infty} \mathbf{u}_{\rm P}(x,y) = (u_\infty, 0), \quad \text{for all } x \in \mathbb{R} \end{cases}$$

This is a nonlinear system of two equations for the two unknown components $u_{\rm P}, v_{\rm P}$ of the velocity $\mathbf{u}_{\rm P}$. The first differential equation in $(P_{\rm P})$ is a parabolic equation, in contrast to the elliptic equation in $(P_{\rm NS})$. From Prandtl's work it is known that the solution of $(P_{\rm P})$ is a good approximation to the solution of $(P_{\rm NS})$ in a subdomain excluding the leading edge region, provided that the flow remains laminar and that no separation occurs. Because of the parabolic nature of the problem $(P_{\rm P})$, the solution at all points in the open half plane to the left of the leading edge is $\mathbf{u}_{\rm P} = (u_\infty, 0)$.

2 Blasius' solution

The classical approach of Blasius [2], which is described in [6], shows that in the open quarter plane $\{(x,y) : x > 0, y > 0\}$ a self–similar solution $\mathbf{u}_{\rm B} = (u_{\rm B}, v_{\rm B})$ of $(P_{\rm P})$ can be written in the form

$$u_{\rm B}(x,y) = u_\infty f'(\eta) \tag{1a}$$

$$v_{\rm B}(x,y) = \frac{1}{2}\sqrt{\frac{2u_\infty}{xRe}}(\eta f'(\eta) - f(\eta)) \tag{1b}$$

where

$$\eta = y\sqrt{u_\infty Re/2x} \tag{1c}$$

and the function f is the solution of the Blasius problem

$$(P_{\rm B}) \begin{cases} \text{Find} f \in C^3([0,\infty)) \text{ such that for all } \eta \in (0,\infty) \\ \\ f'''(\eta) + f(\eta)f''(\eta) = 0 \\ \\ f(0) = f'(0) = 0, \quad \lim_{\eta\to\infty} f'(\eta) = 1. \end{cases}$$

In what follows we refer to $\mathbf{u}_{\rm B}$ as the Blasius solution of $(P_{\rm P})$. In [3] the Blasius problem $(P_{\rm B})$ is solved numerically for the function f, and the relations 1a and 1b are then used to construct the Blasius solution $\mathbf{u}_{\rm B}$ of $(P_{\rm P})$. The approach in [3] differs from the standard one in that Re–uniform analytic approximations are constructed with guaranteed accuracy to the solution $\mathbf{u}_{\rm P}$ of $(P_{\rm P})$ and its scaled first derivatives for all values of Re at all points of the domain Ω. This computed Blasius solution $\mathbf{U}_{\rm B}$ is used in subsequent sections to estimate errors in the numerical method used in this paper.

3 Prandtl problem in a finite domain

We construct a numerical method to compute directly pointwise–accurate and parameter–uniform numerical approximations to the solution of the Prandtl problem $(P_{\rm P})$ in a finite rectangular domain $\Omega = (a,A) \times (0,B)$ on one side of the plate, which is a fixed distance to the right of the leading edge of the plate. By symmetry this domain can be taken on either side of the plate and it can be as close to the leading edge and as large as desired, provided that its location and size are independent of the Reynolds number. We denote the boundary by $\Gamma = \Gamma_{\rm L} \cup \Gamma_{\rm R} \cup \Gamma_{\rm T} \cup \Gamma_{\rm B}$ where $\Gamma_{\rm L}$, $\Gamma_{\rm R}$, $\Gamma_{\rm T}$ and $\Gamma_{\rm B}$ denote, respectively the left–hand, right–hand, top and bottom edges of Ω. In our numerical computations we use the specific values

$$u_\infty = 1.0, \quad a = 0.1, \quad A = 1.1, \quad B = 1 \quad \text{and} \quad Re \in [1,\infty).$$

We use the computed Blasius solution from [3] to give the required boundary conditions on $\Gamma_{\rm T}$ and inflow conditions on $\Gamma_{\rm L}$. Having found a numerical solution with this direct method, we investigate its error by comparing it with the computed Blasius solution $U_{\rm B}$ obtained in [3].

It is convenient, in what follows, to introduce the notation $\varepsilon = \frac{1}{Re}$, where small ε will now indicate high Reynolds number. We consider the following problem:

$$(P_\varepsilon) \begin{cases} \text{Find } \mathbf{u}_\varepsilon = (u_\varepsilon, v_\varepsilon) \text{ such that for all } (x,y) \in \Omega \\ \\ -\varepsilon \frac{\partial^2 u_\varepsilon(x,y)}{\partial y^2} + \mathbf{u}_\varepsilon \cdot \nabla u_\varepsilon(x,y) = 0 \\ \\ \nabla \cdot \mathbf{u}_\varepsilon(x,y) = 0 \\ \mathbf{u}_\varepsilon = \mathbf{0} \quad \text{on} \quad \Gamma_{\rm B} \\ u_\varepsilon = u_{\rm P} \quad \text{on} \quad \Gamma_{\rm L} \cup \Gamma_{\rm T} \end{cases}$$

where $\mathbf{u}_{\rm P}$ is the exact solution of $(P_{\rm P})$. Since we take the boundary conditions in (P_ε) to be the appropriate values of $u_{\rm P}$ on $\Gamma_{\rm L} \cup \Gamma_{\rm T} \cup \Gamma_{\rm B}$ and of $v_{\rm P}$ on $\Gamma_{\rm B}$, it follows that on the finite rectangle $\overline{\Omega}$ the solution $\mathbf{u}_\varepsilon$ of (P_ε) is equal to the solution $\mathbf{u}_{\rm P}$ of $(P_{\rm P})$.

4 Nonlinear finite difference method

We now construct a direct numerical method for solving (P_ε). This comprises a standard upwind finite difference operator on an appropriate piecewise uniform fitted mesh of the kind described in [4]. Because the computational domain is rectangular, the piecewise uniform fitted rectangular mesh $\Omega_\varepsilon^{\mathbf{N}}$ is the tensor product of one dimensional meshes. Since there is just one boundary layer in the solution, we can take a uniform mesh in the direction of the time–like x–axis and a piecewise uniform fitted mesh in the direction of the y–axis. Taking the tensor product of these meshes we have $\overline{\Omega}_\varepsilon^{\mathbf{N}} = \overline{\Omega}_u^{N_x} \times \overline{\Omega}_\varepsilon^{N_y}$, where $\mathbf{N} = (N_x, N_y)$, $\overline{\Omega}_u^{N_x}$ is a uniform mesh with N_x mesh intervals on the interval $[a, A]$ of the x–axis, and $\overline{\Omega}_\varepsilon^{N_y}$ is a piecewise uniform fitted mesh with N_y mesh intervals on the interval $[0, B]$ of the y–axis, such that the subinterval $[0, \sigma]$ and the subinterval $[\sigma, B]$ are both subdivided into $\frac{1}{2}N_y$ uniform mesh intervals.

By analogy with the case of parabolic boundary layers arising in linear problems, we define the transition parameter σ to be

$$\sigma = \min\{\frac{1}{2}B,\ \sqrt{\varepsilon}\ln N_y\}.$$

The choice here of $\sqrt{\varepsilon}$ can be motivated either from *a priori* estimates of the derivatives of the solution $\mathbf{u}_\varepsilon$ or from the asymptotic analysis in [6].

Using the above piecewise uniform fitted mesh $\Omega_\varepsilon^{\mathbf{N}}$ the problem (P_ε) is discretized by the following nonlinear system of upwind finite difference equations for the approximate velocity components $\mathbf{U}_\varepsilon = (U_\varepsilon, V_\varepsilon)$

$$(P_\varepsilon^{\mathbf{N}}) \begin{cases} \text{Find } \mathbf{U}_\varepsilon = (U_\varepsilon, V_\varepsilon) \text{ such that for all } (x_i, y_j) \in \Omega_\varepsilon^{\mathbf{N}} \\ -\varepsilon \delta_y^2 U_\varepsilon(x_i, y_j) + \big(\mathbf{U}_\varepsilon \cdot \mathbf{D}^-\big) U_\varepsilon(x_i, y_j) = 0 \\ \big(\mathbf{D}^- \cdot \mathbf{U}_\varepsilon\big)(x_i, y_j) = 0 \\ \mathbf{U}_\varepsilon = \mathbf{0} \quad \text{on} \quad \Gamma_{\mathrm{B}} \\ U_\varepsilon = U_{\mathrm{B}} \text{ on} \quad \Gamma_{\mathrm{L}} \cup \Gamma_{\mathrm{T}} \end{cases}$$

where $\mathbf{D}^- = (D_x^-, D_y^-)$, D_x^-, D_y^- are standard backward difference operators, and δ_y^2 is a standard central difference operator. We note that in $(P_\varepsilon^{\mathbf{N}})$ we use the known approximate boundary values U_{B} on $\Gamma_{\mathrm{L}} \cup \Gamma_{\mathrm{T}}$ to replace the unknown exact boundary values u_{P}, where $\mathbf{U}_{\mathrm{B}}$ is the Blasius solution of the Prandtl problem (P_{P}).

Since $(P_\varepsilon^{\mathbf{N}})$ is a nonlinear finite difference method, it is necessary to prescribe an $\varepsilon-$uniformly convergent nonlinear solver for computing its solution. We note that there are no known theoretical error estimates for the pointwise errors $(\mathbf{U}_\varepsilon - \mathbf{u}_\varepsilon)(x_i, y_j)$ in the velocity components, because there are no known theoretical results concerning the convergence of the solutions $\mathbf{U}_\varepsilon$ of $(P_\varepsilon^{\mathbf{N}})$ to the solution $\mathbf{u}_\varepsilon$ of (P_ε).

5 Solution of the nonlinear finite difference method

To find the solution $\mathbf{U}_\varepsilon$ of $(P_\varepsilon^{\mathbf{N}})$ we need to solve a nonlinear system of finite difference equations. We do this with a continuation algorithm, which replaces $(P_\varepsilon^{\mathbf{N}})$ by a sequence of linear systems. From now on, we will assume for simplicity that $N_x = N_y = N$. The algorithm sweeps across the domain $\overline{\Omega}$ from left to right, that is in the same direction as the physical flow. At the i^{th} stage of the sweep, we compute the values of $\mathbf{U}_\varepsilon$ on $X_i = \{(x_i, y_j), 1 \le j \le N\}$ assuming that values of $\mathbf{U}_\varepsilon$ are known on X_{i-1}. To achieve this we employ an iterative method to solve successively both a nonlinear system for U_ε and a linear system for V_ε.

For each i, $1 \le i \le N$, we linearise the nonlinear system for U_ε on X_i by introducing the sequence of linear problems

$$(-\varepsilon \delta_y^2 U_\varepsilon^m + (\mathbf{U}_\varepsilon^{m-1} \cdot \mathbf{D}^-) U_\varepsilon^m)(x_i, y_j) = 0, \quad 1 \le j \le N-1$$

where $\{U_\varepsilon^m(x_i, y_j),\ 1 \le j \le N-1\}$ are the unknown values of the m^{th} iterate and $\{\mathbf{U}^{m-1}(x_i, y_j),\ 1 \le j \le N-1\}$ are the known values of the $(m-1)^{th}$ iterate. In order to solve this system on X_i we need values of U_ε on X_{i-1}, boundary values for U_ε^m at

points of $\Gamma_{\rm B} \cup \Gamma_{\rm T}$ and an initial guess $\mathbf{U}_\varepsilon^0$ on X_i. The required values on $\Gamma_{\rm B} \cup \Gamma_{\rm T}$ are taken to be the given boundary conditions for U_ε on $\Gamma_{\rm B} \cup \Gamma_{\rm T}$, and in general, we take as the initial guess $\mathbf{U}_\varepsilon^0$ on X_i the value of the final iterate on X_{i-1}. The initial guess $\mathbf{U}_\varepsilon^0$ on X_1 is taken to be the prescribed boundary conditions for U_ε on $\Gamma_{\rm L}$ and V_ε^0 is taken to be zero.

Having solved the tridiagonal system for U_ε on X_i, we then find V_ε by solving the linear system

$$\mathbf{D}^- \cdot \mathbf{U}_\varepsilon^m(x_i, y_j) = 0, \quad 1 \le j \le N.$$

for the unknown values $\{V_\varepsilon(x_i, y_j),\ 1 \le j \le N\}$, where we take $V_\varepsilon = 0$ on $\Gamma_{\rm B}$. Note that this requires only the given initial condition for V_ε on $\Gamma_{\rm B}$.

We continue this process until the change between two successive iterates for the scaled velocity $(U_\varepsilon^m, \frac{1}{\sqrt{\varepsilon}} V_\varepsilon^m)$ is less than a specified tolerance tol, that is

$$\max(|U_\varepsilon^m - U_\varepsilon^{m-1}|_{\Omega_\varepsilon^N}, \frac{1}{\sqrt{\varepsilon}} |V_\varepsilon^m - V_\varepsilon^{m-1}|_{\Omega_\varepsilon^N} \le tol$$

where we take $tol = 10^{-6}$. We denote by M the value of m for which this occurs. When this tolerance is achieved, we proceed to the next X_i and use the solution $\mathbf{U}_\varepsilon^M$

as the initial guess there. The resulting algorithm may be written as:

$$(A_\varepsilon^{\mathbf{N}})\ \begin{cases} \text{With } U_\varepsilon^M = U_{\mathrm{B}} \text{ on } \Gamma_{\mathrm{L}}, \\ \\ \text{for each } X_i, 1 \le i \le N, \text{ use the initial guess } \mathbf{U}_\varepsilon^0|_{X_i} = \mathbf{U}_\varepsilon^M|_{X_{i-1}} \\ \\ \text{and for } \ m = 1, \ldots, M \ \text{ solve the following} \\ \text{two point boundary value problem for } U_\varepsilon^m(x_i, y_j) \\ \\ (-\varepsilon\delta_y^2 + \mathbf{U}_\varepsilon^{m-1} \cdot \mathbf{D}^-)U_\varepsilon^m(x_i, y_j) = 0, \quad x_i \in X_i \\ \\ \text{with } U_\varepsilon^m = U_{\mathrm{B}} \text{ on } \Gamma_{\mathrm{B}} \cup \Gamma_{\mathrm{T}}, \\ \\ \text{and } V_\varepsilon^0|_{X_1} = 0. \\ \\ \text{Also solve the initial value problem for } V_\varepsilon^m(x_i, y_j) \\ \\ (\mathbf{D}^- \cdot \mathbf{U}_\varepsilon^m)(x_i, y_j) = 0, \\ \\ \text{with } V_\varepsilon^m = 0 \text{ on } \Gamma_{\mathrm{B}}. \\ \\ \text{Continue to iterate between the equations for } \mathbf{U}_\varepsilon^m \text{ until } m = M, \\ \text{where } M \text{ is such that} \\ \\ \max(|U_\varepsilon^M - U_\varepsilon^{M-1}|_{\overline{\Omega}_\varepsilon^N}, \frac{1}{\sqrt{\varepsilon}}|V_\varepsilon^M - V_\varepsilon^{M-1}|_{\overline{\Omega}_\varepsilon^N}) \le tol. \end{cases}$$

For notational simplicity, we suppress explicit mention of the iteration superscript M in what follows, and we write simply $\mathbf{U}_\varepsilon$ for the solution of $(A_\varepsilon^{\mathbf{N}})$. Graphs of the solution $\mathbf{U}_\varepsilon$ of the direct method $(A_\varepsilon^{\mathbf{N}})$ with $N = 32$ for $\varepsilon = 1$, 0.01 and $\varepsilon = 0.00001$ respectively are shown in Figs. 1, 2 and 3. In the next section we show computationally that this direct algorithm gives pointwise–accurate parameter–uniform approximations to the scaled velocity $(u_\varepsilon, \frac{1}{\sqrt{\varepsilon}}u_\varepsilon)$ and its scaled derivatives.

We also approximate the scaled partial derivatives $\dfrac{\partial u_\varepsilon}{\partial x}$, $\varepsilon^{1/2}\dfrac{\partial u_\varepsilon}{\partial y}$ and $\varepsilon^{-1/2}\dfrac{\partial v_\varepsilon}{\partial x}$ by the correspondingly scaled discrete derivatives $D_x^- U_\varepsilon$, $\varepsilon^{1/2} D_y^- U_\varepsilon$ and $\varepsilon^{-1/2} D_x^- V_\varepsilon$, noting that $\dfrac{\partial u_\varepsilon}{\partial x} = -\dfrac{\partial v_\varepsilon}{\partial y}$ and $D_x^- U_\varepsilon = -D_y^- V_\varepsilon$. Graphs of these computed scaled discrete derivatives are given for $N = 32$ and two values of ε in Figs. 4, 5, and 6.

It is also of interest to investigate whether or not the number of iterations required for convergence of the nonlinear solver is independent of ε. We note from Table 1 that the number of iterations per time-like level X_i tends to just a few iterations for i

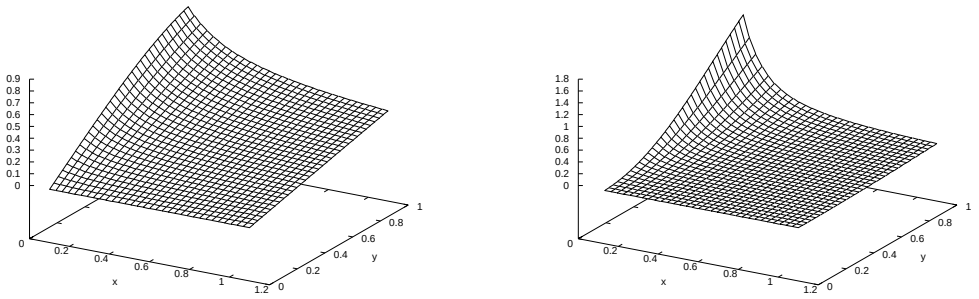

Figure 1: Graphs of $(U_\varepsilon, \varepsilon^{-1/2}V_\varepsilon)$ given by $(A_\varepsilon^{\mathbf{N}})$ for $\varepsilon = 1.0$ and $N = 32$.

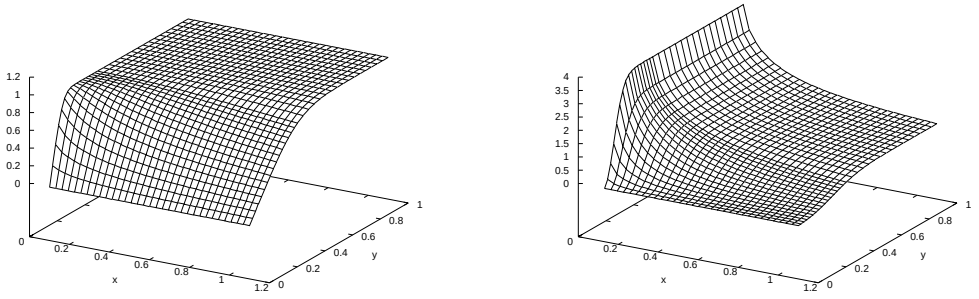

Figure 2: Graphs of $(U_\varepsilon, \varepsilon^{-1/2}V_\varepsilon)$ given by $(A_\varepsilon^{\mathbf{N}})$ for $\varepsilon = 0.01$ and $N = 32$.

large, which means that the method becomes equivalent essentially to a direct rather than an iterative method.

6 Computed error estimates using the Blasius solution

In this section we estimate the error in the numerical approximations $(U_\varepsilon, \sqrt{Re}V_\varepsilon)$ given by the method $(A_\varepsilon^{\mathbf{N}})$. We begin by observing that

$$\begin{aligned} |U_\varepsilon - u_{\mathrm{P}}|_{\Omega_\varepsilon^N} &= |U_\varepsilon - u_{\mathrm{B}}|_{\Omega_\varepsilon^N} \\ &\leq |U_\varepsilon - U_{\mathrm{B}}|_{\Omega_\varepsilon^N} + |U_{\mathrm{B}} - u_{\mathrm{B}}|_{\Omega_\varepsilon^N} \qquad (2) \\ \sqrt{Re}|V_\varepsilon - v_{\mathrm{P}}|_{\Omega_\varepsilon^N} &= \varepsilon^{-1/2}|V_\varepsilon - v_{\mathrm{B}}|_{\Omega_\varepsilon^N} \\ &\leq \varepsilon^{-1/2}|V_\varepsilon - V_{\mathrm{B}}|_{\Omega_\varepsilon^N} + \varepsilon^{-1/2}|V_{\mathrm{B}} - v_{\mathrm{B}}|_{\Omega_\varepsilon^N}, \qquad (3) \end{aligned}$$

where $\mathbf{U}_\varepsilon = (U_\varepsilon, V_\varepsilon)$ is the solution generated by the direct algorithm $(A_\varepsilon^{\mathbf{N}})$ on the mesh $\Omega_\varepsilon^{\mathbf{N}}$ with $\mathbf{N} = (N, N)$, $\mathbf{u}_{\mathrm{B}} = (u_{\mathrm{B}}, v_{\mathrm{B}})$ is the exact solution of the Prandtl

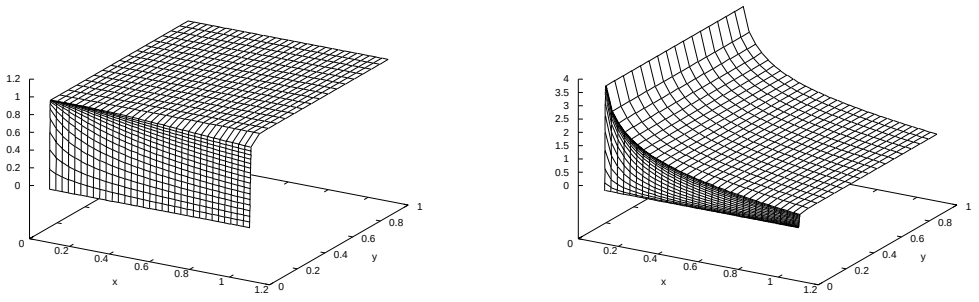

Figure 3: Graphs of $(U_\varepsilon, \varepsilon^{-1/2}V_\varepsilon)$ given by $(A_\varepsilon^{\mathbf{N}})$ for $\varepsilon = 0.00001$ and $N = 32$.

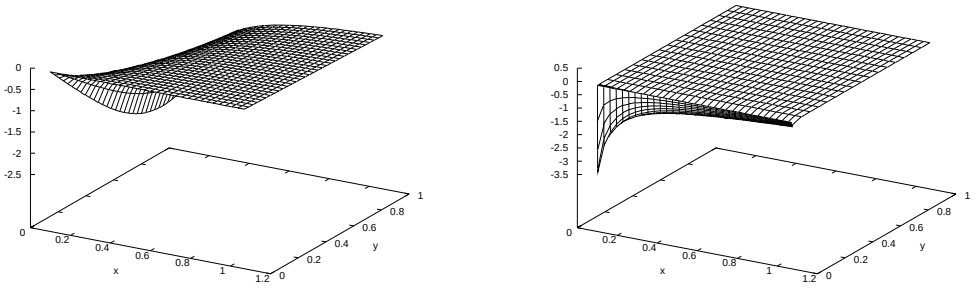

Figure 4: Graph of $D_x^- U_\varepsilon$ given by $(A_\varepsilon^{\mathbf{N}})$ with $N = 32$ and $\varepsilon = 1.0$ and 0.00001 respectively.

problem constructed from the Blasius formulae 1a and 1b, and $\mathbf{U}_{\mathrm{B}} = (U_{\mathrm{B}}, V_{\mathrm{B}})$ is the numerical solution of the Blasius equation obtained in [3] on a mesh with 8192 intervals. Since the terms on the right–hand side of (2)–(3) can be estimated by numerical experiments, it follows that we can obtain experimental estimates for the errors in the numerical approximations generated by $(A_\varepsilon^{\mathbf{N}})$ to the solutions of (P_ε), even though at present no theoretical error analysis is available for this numerical method.

We now consider the relative magnitude of the two terms on the right–hand side of (2) and (3). The first terms are the scaled maximum pointwise differences $\|U_\varepsilon - U_{\mathrm{B}}\|_{\overline{\Omega}_\varepsilon^N}$ and $\varepsilon^{-1/2}\|V_\varepsilon - V_{\mathrm{B}}\|_{\overline{\Omega}_\varepsilon^N}$. These quantities are easy to determine numerically from the solution $\mathbf{U}_\varepsilon$ of $(A_\varepsilon^{\mathbf{N}})$ found in the previous section and the solution $\mathbf{U}_{\mathrm{B}}$ computed in [3]. The results are given in Tables 2 and 3 respectively for various values of ε and N. The other terms on the right–hand sides of (2)–(3) are the scaled maximum pointwise errors $|U_{\mathrm{B}} - u_{\mathrm{B}}|_{\Omega_\varepsilon^N}$ and $\varepsilon^{-1/2}|V_{\mathrm{B}} - v_{\mathrm{B}}|_{\Omega_\varepsilon^N}$. We know from [3] that the first term on the right–hand side of both (2) and (3) dominates the second term, and thus the first term on the right–hand side of (2)–(3) may be taken to approximate the true error

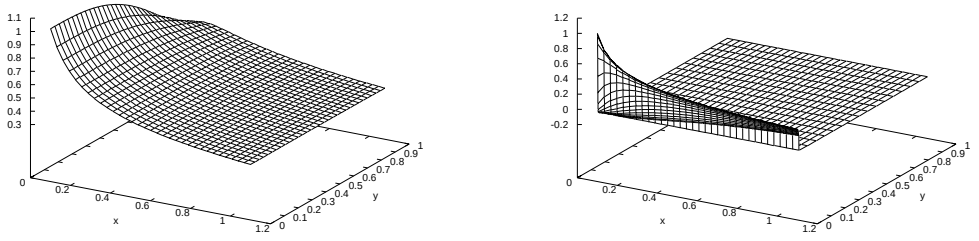

Figure 5: Graph of $\varepsilon^{1/2} D_y^- U_\varepsilon$ given by $(A_\varepsilon^{\mathbf{N}})$ with $N = 32$ and $\varepsilon = 1.0$ and 0.00001 respectively.

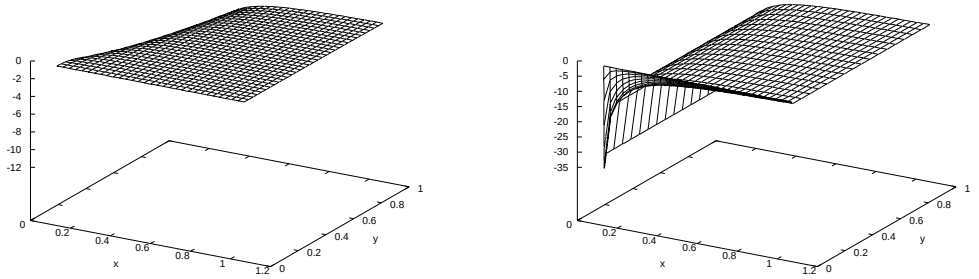

Figure 6: Graph of $\varepsilon^{-1/2} D_x^- V_\varepsilon$ given by $(A_\varepsilon^{\mathbf{N}})$ with $N = 32$ and $\varepsilon = 1.0$ and 0.00001 respectively.

at least to experimental accuracy. Graphs of these first terms are shown in Figs. 7, 8 and 9 for $N = 32$ and $\varepsilon = 1.0, 0.01$ and 0.00001, respectively.

We now estimate the order of convergence of the numerical approximations $\mathbf{U}_\varepsilon$, by introducing the computed orders of convergence $p^N_{\varepsilon,\mathrm{comp}}$ and p^N_{comp}

$$p^N_{\varepsilon,\mathrm{comp}} = \log_2 \frac{|U^N_\varepsilon - U_{\mathrm{B}}|_{\Omega^N_\varepsilon}}{|U^{2N}_\varepsilon - U_{\mathrm{B}}|_{\Omega^{2N}_\varepsilon}}$$

$$p^N_{\mathrm{comp}} = \log_2 \frac{\max_\varepsilon |U^N_\varepsilon - U_{\mathrm{B}}|_{\Omega^N_\varepsilon}}{\max_\varepsilon |U^{2N}_\varepsilon - U_{\mathrm{B}}|_{\Omega^{2N}_\varepsilon}}$$

for the first component, with corresponding definitions for the scaled second component. The values of the $p^N_{\varepsilon,\mathrm{comp}}$ and p^N_{comp} for the scaled components of $\mathbf{U}_\varepsilon$ are given in Tables 4 and 5 respectively. These tables suggest an ε-uniform order of at least 0.8 and 0.7, respectively.

Table 1: Number of one dimensional linear solves per level X_i for convergence of $(A_\varepsilon^{\mathbf{N}})$ for various values of ε and N.

ε	8	16	32	64	128	256	512
2^0	7	8	9	10	10	10	9
2^{-2}	17	16	16	14	13	12	11
2^{-4}	34	24	19	16	15	13	12
2^{-6}	36	28	23	19	16	14	12
2^{-8}	35	28	23	19	16	14	13
2^{-10}	35	28	23	19	16	14	13
2^{-12}	36	28	23	19	16	14	13
2^{-14}	36	28	23	19	16	14	13
2^{-16}	36	29	23	19	16	14	13
2^{-18}	36	29	23	19	16	14	13
2^{-20}	36	29	23	19	16	14	13

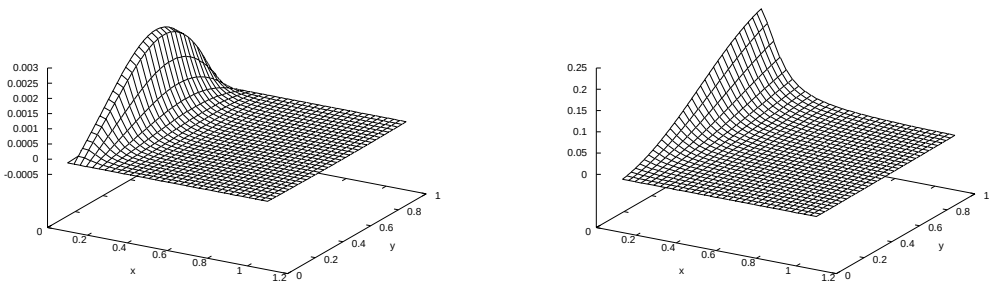

Figure 7: Graphs of $U_\varepsilon - U_{\rm B}$ and $\varepsilon^{-1/2}(V_\varepsilon - V_{\rm B})$ where $\mathbf{U}_\varepsilon = (U_\varepsilon, V_\varepsilon)$ is given by $(A_\varepsilon^{\mathbf{N}})$ for $\varepsilon = 1.0$ and $N = 32$.

We now apply the same argument as above to estimate the maximum pointwise error in the scaled discrete derivatives of $\mathbf{U}_\varepsilon$. As before we examine the relative magnitude of both terms on the right–hand side of the analogous expressions to (2)–(3). We show the values of the computed discrete derivatives $\|D_x^- U_\varepsilon - D_x U_{\rm B})\|_{\overline{\Omega}_\varepsilon^N}$ and $\sqrt{\varepsilon}\|D_y^- U_\varepsilon - D_y U_{\rm B}\|_{\overline{\Omega}_\varepsilon^N}$ in Tables 6 and 7 for various values of ε and N. Again, the values of $\|D_x^- U_\varepsilon - D_x U_{\rm B})\|_{\overline{\Omega}}$ are identical to those of $\|D_y^- V_\varepsilon - D_y V_{\rm B})\|_{\overline{\Omega}}$ and so no separate table is required. From Tables 9 and 8 we see that the smallest value of $\sqrt{\varepsilon}\|D_y^- U_\varepsilon - D_y U_{\rm B})\|_{\overline{\Omega}_\varepsilon^N}$ is 0.139×10^{-2} and of $\|D_x^- U_\varepsilon - D_x U_{\rm B})\|_{\overline{\Omega}_\varepsilon^N}$ is 0.178×10^{-1}. The corresponding computed orders of convergence $p^N_{\varepsilon,\rm comp}$ and $p^N_{\rm comp}$ for $D_x^- U_\varepsilon$ and $D_y^- U_\varepsilon$ are given in Tables 8 and 9 respectively. The entries indicate that the ε–uniform orders of convergence are at least 0.6 for all $N \geq 32$.

The qualitative behaviour of the error in the computed scaled discrete derivatives can be seen from the graphs of $D_x^- U_\varepsilon - D_x U_{\rm B}$, $\sqrt{\varepsilon}(D_y^- U_\varepsilon - D_y U_{\rm B})$ and $\varepsilon^{-1/2}(D_x^- V_\varepsilon - D_x V_{\rm B})$ which are displayed in Figs. 10, 11 and 12. We see from the graph of $\varepsilon^{-1/2}(D_x^- V_\varepsilon - D_x V_{\rm B})$ in Fig. 12 and from the entries in Table 10 that there is

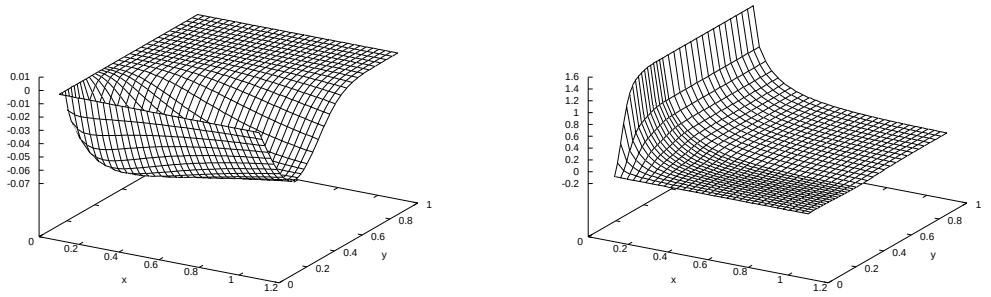

Figure 8: Graphs of $U_\varepsilon - U_{\rm B}$ and $\varepsilon^{-1/2}(V_\varepsilon - V_{\rm B})$ where $\mathbf{U}_\varepsilon = (U_\varepsilon, V_\varepsilon)$ is given by $(A_\varepsilon^{\mathbf{N}})$ for $\varepsilon = 0.01$ and $N = 32$.

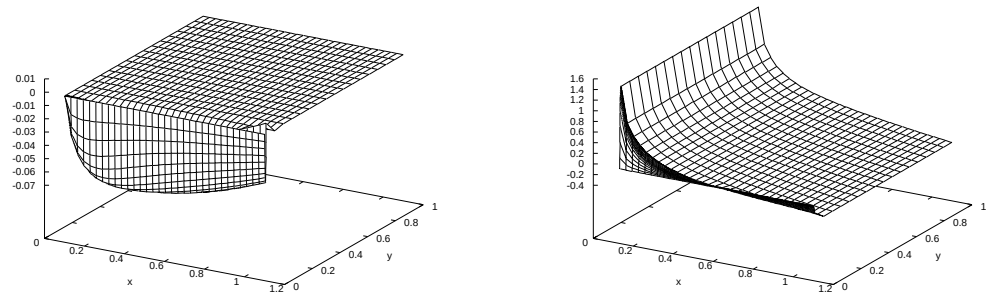

Figure 9: Graphs of $U_\varepsilon - U_{\rm B}$ and $\varepsilon^{-1/2}(V_\varepsilon - V_{\rm B})$ where $\mathbf{U}_\varepsilon = (U_\varepsilon, V_\varepsilon)$ is given by $(A_\varepsilon^{\mathbf{N}})$ for $\varepsilon = 0.00001$ and $N = 32$.

a singularity in $\varepsilon^{-1/2}\dfrac{\partial v_\varepsilon}{\partial x}$ in a neighbourhood of the corner $C_{\rm TL} = (0.1, 1)$. This singularity is not resolved by method $(A_\varepsilon^{\mathbf{N}})$. However, in [3] further numerical results are presented which indicate that the computed scaled discrete derivatives $\varepsilon^{-1/2}D_x^- V_\varepsilon$ appear to converge ε–uniformly to the corresponding scaled derivative $\varepsilon^{-1/2}\dfrac{\partial v_\varepsilon}{\partial x}$ in subdomains which exclude a sufficiently large neighbourhood of this corner.

In summary, we have shown experimentally that method $(A_\varepsilon^{\mathbf{N}})$ produces ε–uniform approximations to the scaled components of $\mathbf{u}_{\rm P}$ and its scaled derivatives.

References

[1] Acheson D. J. (1990). *Elementary Fluid Dynamics.* Oxford University Press.

[2] Blasius H. (1908). Grenzschichten in Flüssigkten mit Kleiner Reibung. *Z. Math. u. Phys.*, **56**, 1–37; Engl. trans. in NACA TM 1256.

Table 2: Computed maximum pointwise difference $\|U_\varepsilon - U_{\rm B}\|_{\overline{\Omega}_\varepsilon^N}$ where U_ε is given by $(A_\varepsilon^{\mathbf{N}})$ for various values of ε and N.

ε	8	16	32	64	128	256	512
2^0	0.420D-02	0.459D-02	0.287D-02	0.166D-02	0.898D-03	0.450D-03	0.211D-03
2^{-2}	0.509D-01	0.248D-01	0.124D-01	0.622D-02	0.312D-02	0.157D-02	0.792D-03
2^{-4}	0.207D+00	0.787D-01	0.352D-01	0.167D-01	0.817D-02	0.404D-02	0.202D-02
2^{-6}	0.220D+00	0.115D+00	0.616D-01	0.326D-01	0.156D-01	0.762D-02	0.378D-02
2^{-8}	0.213D+00	0.114D+00	0.616D-01	0.340D-01	0.189D-01	0.105D-01	0.581D-02
.	.	.	.	.	.	.	.
.	.	.	.	.	.	.	.
.	.	.	.	.	.	.	.
2^{-20}	0.208D+00	0.113D+00	0.616D-01	0.340D-01	0.189D-01	0.105D-01	0.581D-02

Table 3: Computed maximum pointwise difference $\varepsilon^{-1/2}\|V_\varepsilon - V_{\rm B}\|_{\overline{\Omega}_\varepsilon^N}$ where V_ε is given by $(A_\varepsilon^{\mathbf{N}})$ for various values of ε and N.

ε	8	16	32	64	128	256	512
2^0	0.533D+00	0.374D+00	0.213D+00	0.108D+00	0.536D-01	0.268D-01	0.142D-01
2^{-2}	0.106D+01	0.677D+00	0.371D+00	0.194D+00	0.101D+00	0.531D-01	0.287D-01
2^{-4}	0.396D+01	0.163D+01	0.763D+00	0.382D+00	0.197D+00	0.104D+00	0.562D-01
2^{-6}	0.457D+01	0.271D+01	0.154D+01	0.849D+00	0.416D+00	0.215D+00	0.114D+00
2^{-8}	0.448D+01	0.269D+01	0.154D+01	0.893D+00	0.523D+00	0.309D+00	0.183D+00
.	.	.	.	.	.	.	.
.	.	.	.	.	.	.	.
.	.	.	.	.	.	.	.
2^{-20}	0.424D+01	0.267D+01	0.154D+01	0.893D+00	0.523D+00	0.309D+00	0.183D+00

[3] Farrell, P.A., Miller J. J. H., O'Riordan E. and Shishkin G.I. *A Robust Computational Technique for Boundary Layers.* (submitted for publication.)

[4] Miller J. J. H., O'Riordan E. and Shishkin G.I. (1996). *Fitted Numerical Methods for Singular Perturbation Problems.* World Scientific Publishing Co.. Singapore.

[5] Prandtl L. (1904). Über Flussigkeitsbewegung bei sehr kleiner Reibung. *Proc. III Intern. Congr. Math., Heidelberg.*

[6] Schlichting H. (1979). *Boundary Layer Theory*, 7th edition, McGraw–Hill, New York.

Table 4: Computed orders of convergence $p^N_{\varepsilon,\mathrm{comp}}$ and p^N_{comp} for $U_\varepsilon - U_{\mathrm{B}}$ where U_ε is given by $(A^{\mathbf{N}}_\varepsilon)$ for various values of ε and N.

ε	8	16	32	64	128	256
2^0	-0.13	0.68	0.78	0.89	1.00	1.09
2^{-2}	1.03	1.00	0.99	1.00	0.99	0.98
2^{-4}	1.39	1.16	1.07	1.03	1.01	1.00
2^{-6}	0.94	0.90	0.92	1.07	1.03	1.01
2^{-8}	0.90	0.89	0.86	0.85	0.85	0.85
.	.	.	.	.	.	.
.	.	.	.	.	.	.
.	.	.	.	.	.	.
2^{-20}	0.88	0.88	0.86	0.85	0.85	0.85
p^N_{comp}	0.94	0.90	0.86	0.85	0.85	0.85

Table 5: Computed orders of convergence $p^N_{\varepsilon,\mathrm{comp}}$ and p^N_{comp} for $\varepsilon^{-1/2}(V_\varepsilon - V_{\mathrm{B}})$ where V_ε is given by $(A^{\mathbf{N}}_\varepsilon)$ for various values of ε and N.

ε	8	16	32	64	128	256
2^0	0.51	0.81	0.98	1.01	1.00	0.92
2^{-2}	0.65	0.87	0.94	0.95	0.92	0.89
2^{-4}	1.28	1.09	1.00	0.96	0.91	0.89
2^{-6}	0.76	0.81	0.86	1.03	0.95	0.92
2^{-8}	0.73	0.80	0.79	0.77	0.76	0.76
.	.	.	.	.	.	.
.	.	.	.	.	.	.
.	.	.	.	.	.	.
2^{-20}	0.67	0.79	0.79	0.77	0.76	0.76
p^N_{comp}	0.76	0.81	0.79	0.77	0.76	0.76

Table 6: Computed maximum pointwise difference $\|D^-_x U_\varepsilon - D_x U_{\mathrm{B}}\|_{\overline{\Omega}^N_\varepsilon}$ where U_ε is given by $(A^{\mathbf{N}}_\varepsilon)$ for various values of ε and N.

ε	8	16	32	64	128	256	512
2^0	0.614D+00	0.444D+00	0.256D+00	0.130D+00	0.668D-01	0.344D-01	0.178D-01
2^{-2}	0.900D+00	0.633D+00	0.372D+00	0.201D+00	0.105D+00	0.556D-01	0.307D-01
2^{-4}	0.189D+01	0.114D+01	0.650D+00	0.360D+00	0.194D+00	0.105D+00	0.573D-01
2^{-6}	0.198D+01	0.167D+01	0.121D+01	0.759D+00	0.397D+00	0.210D+00	0.113D+00
2^{-8}	0.197D+01	0.167D+01	0.121D+01	0.798D+00	0.496D+00	0.300D+00	0.180D+00
.	.	.	.	.	.	.	.
.	.	.	.	.	.	.	.
.	.	.	.	.	.	.	.
2^{-20}	0.195D+01	0.167D+01	0.121D+01	0.798D+00	0.496D+00	0.300D+00	0.180D+00

Table 7: Computed maximum pointwise difference $\|\sqrt{\varepsilon}(D_y U_\varepsilon - D_y^- U_{\rm B})\|_{\overline{\Omega}_\varepsilon^N}$ where U_ε is given by $(A_\varepsilon^{\mathbf{N}})$ for various values of ε and N.

ε	8	16	32	64	128	256	512
2^0	0.703D-01	0.357D-01	0.180D-01	0.914D-02	0.471D-02	0.249D-02	0.139D-02
2^{-2}	0.193D+00	0.111D+00	0.603D-01	0.315D-01	0.162D-01	0.819D-02	0.414D-02
2^{-4}	0.266D+00	0.140D+00	0.703D-01	0.357D-01	0.180D-01	0.914D-02	0.471D-02
2^{-6}	0.279D+00	0.192D+00	0.118D+00	0.703D-01	0.357D-01	0.180D-01	0.914D-02
2^{-8}	0.279D+00	0.192D+00	0.118D+00	0.733D-01	0.432D-01	0.248D-01	0.141D-01
.	.	.	.	.	.	.	.
.	.	.	.	.	.	.	.
.	.	.	.	.	.	.	.
2^{-20}	0.279D+00	0.192D+00	0.118D+00	0.733D-01	0.432D-01	0.248D-01	0.141D-01

Table 8: Computed orders of convergence $p^N_{\varepsilon,\rm comp}$ and $p^N_{\rm comp}$ for $D_x^- U_\varepsilon - D_x U_{\rm B}$ where U_ε is given by $(A_\varepsilon^{\mathbf{N}})$ for various values of ε and N.

ε	8	16	32	64	128	256
2^0	0.47	0.79	0.98	0.96	0.96	0.95
2^{-2}	0.51	0.76	0.89	0.94	0.92	0.86
2^{-4}	0.73	0.81	0.85	0.89	0.89	0.87
2^{-6}	0.25	0.46	0.68	0.93	0.92	0.90
2^{-8}	0.24	0.46	0.60	0.69	0.72	0.74
.	.	.	.	.	.	.
.	.	.	.	.	.	.
.	.	.	.	.	.	.
2^{-20}	0.22	0.46	0.60	0.69	0.72	0.74
$p^N_{\rm comp}$	0.25	0.46	0.60	0.69	0.72	0.74

Table 9: Computed orders of convergence $p^N_{\varepsilon,\rm comp}$ and $p^N_{\rm comp}$ for $\sqrt{\varepsilon}(D_y^- U_\varepsilon - D_y U_{\rm B})$ where U_ε is given by $(A_\varepsilon^{\mathbf{N}})$ for various values of ε and N.

ε	8	16	32	64	128	256
2^0	0.98	0.99	0.98	0.96	0.92	0.85
2^{-2}	0.79	0.88	0.94	0.96	0.98	0.99
2^{-4}	0.93	1.00	0.98	0.99	0.98	0.96
2^{-6}	0.54	0.71	0.74	0.98	0.99	0.98
2^{-8}	0.54	0.71	0.68	0.77	0.80	0.82
.	.	.	.	.	.	.
.	.	.	.	.	.	.
.	.	.	.	.	.	.
2^{-20}	0.54	0.71	0.68	0.77	0.80	0.82
$p^N_{\rm comp}$	0.54	0.71	0.68	0.77	0.80	0.82

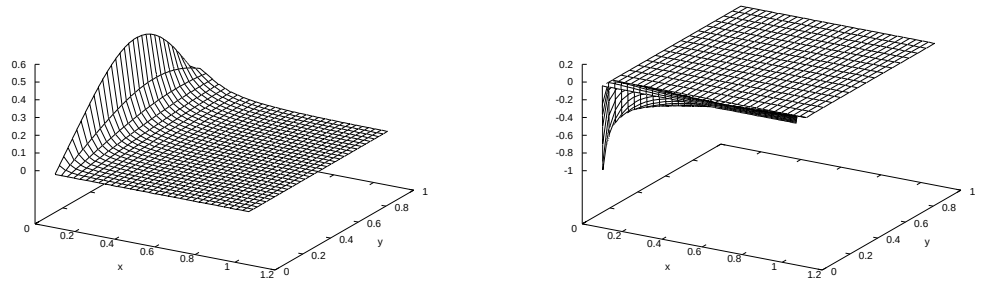

Figure 10: Graphs of $D_x^- U_\varepsilon - D_x U_{\mathrm{B}}$ where U_ε is given by $(A_\varepsilon^{\mathbf{N}})$ with $N = 32$ and $\varepsilon = 1.0$ and 0.00001 respectively.

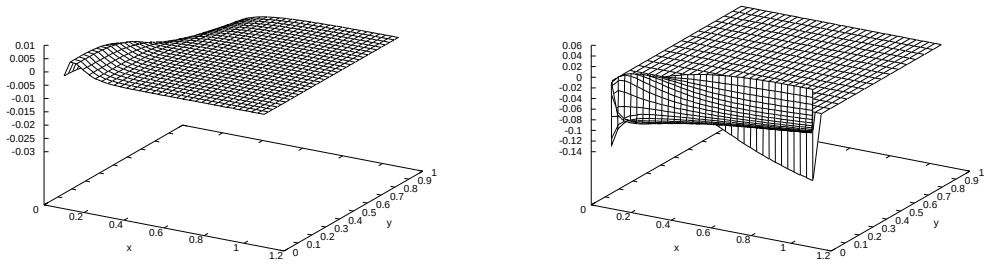

Figure 11: Graphs of $\sqrt{\varepsilon}(D_y^- U_\varepsilon - D_y U_{\mathrm{B}})$ where U_ε is given by $(A_\varepsilon^{\mathbf{N}})$ with $N = 32$ and $\varepsilon = 1.0$ and 0.00001 respectively.

Table 10: Computed maximum pointwise difference $\varepsilon^{-1/2}\|D_x^- V_\varepsilon - \partial_x V_{\mathrm{B}}^{8192}\|_{\overline{\Omega}_\varepsilon^N \setminus (X_1 \cup \Gamma_{\mathrm{L}})}$ where V_ε is generated by method $(A_\varepsilon^{\mathbf{N}})$ applied to problem (P_ε) for various values of ε and N.

ε	8	16	32	64	128	256	512
2^0	0.364D+01	0.406D+01	0.300D+01	0.180D+01	0.113D+01	0.886D+00	0. 922D+00
2^{-2}	0.794D+01	0.647D+01	0.476D+01	0.328D+01	0.232D+01	0.191D+01	0.188D+01
2^{-4}	0.278D+02	0.143D+02	0.989D+01	0.700D+01	0.519D+01	0.428D+01	0.396D+01
2^{-6}	0.311D+02	0.281D+02	0.237D+02	.189D+02	0.130D+02	0.101D+02	0.875D+01
2^{-8}	0.321D+02	0.282D+02	0.237D+02	0.202D+02	0.174D+02	0.158D+02	0.152D+02
.	.	.	.	.	.	.	.
.	.	.	.	.	.	.	.
.	.	.	.	.	.	.	.
2^{-20}	0.342D+02	0.284D+02	0.237D+02	0.202D+02	0.174D+02	0.158D+02	0.152D+02

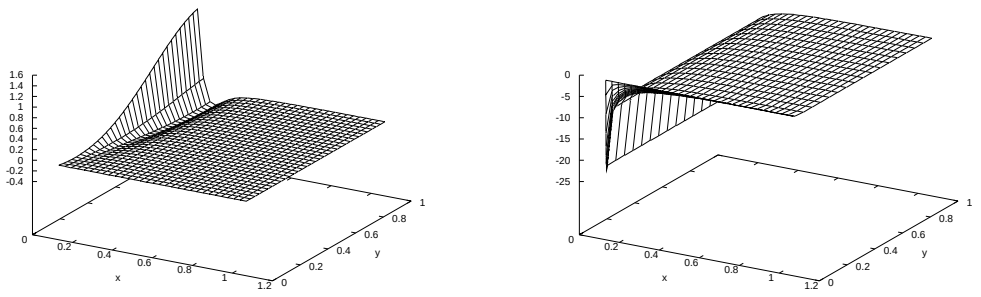

Figure 12: Graph of $\varepsilon^{-1/2}(D_x^- V_\varepsilon - D_x V_{\mathrm{B}})$ where V_ε is given by $(A_\varepsilon^{\mathbf{N}})$ with $N = 32$ and $\varepsilon = 1.0$ and 0.00001 respectively.